# Privacy-Protected Formation Control for Unmanned Surface Vehicles: A Neural Predictor-Based Noncooperative Game Framework

Jinliang Liu, *Senior Member, IEEE*, Zihao Liu, Yan Li, Engang Tian, *Senior Member, IEEE*, and Chen Peng, *Senior Member, IEEE*

***Abstract*—This paper proposes a formation control strategy based on noncooperative game framework for unmanned surface vehicles (USVs) in the presence of eavesdroppers. Firstly, the interactions among USVs during formation control are modeled as a noncooperative game. A privacy-protected estimator is then developed for each USV by employing a twin-network structure, so as to effectively estimate the actions of other USVs while preventing information leakage incurred by eavesdropping attacks. Additionally, a novel neural predictor is designed using an accelerated learning-boosted echo state network (ALESN) to approximate unknown system parameters with enhanced convergence rate and prediction accuracy. On the basis of the estimator and predictor, a distributed formation control method is subsequently devised via seeking the Nash equilibrium of the formulated game. The implementation of the control method only requires local information exchanged between neighboring USVs, and thus the desired computational efficiency and scalability can be achieved. A simulation example is finally provided to validate the effectiveness of the reported privacy-protected formation control approach.**

***Index Terms*—Unmanned surface vehicles (USVs), formation control, twin-network, privacy-protected, noncooperative game, Nash equilibrium.**

## I. Introduction

UNMANNED surface vehicles (USVs) are maritime vessels that can operate autonomously according to predefined objectives or be remotely controlled by human operators, enabling them to carry out various missions at sea independently [1], [2].

Received 18 August 2025; revised 28 November 2025; accepted 4 January 2026. Date of publication 12 January 2026; date of current version 20 July 2026. This work was supported in part by the National Natural Science Foundation of China under Grant 62373252 and in part by the Startup Foundation for Introducing Talent of NUIST under Grant 2024r063. The review of this article was coordinated by Prof. Shahid Mumtaz. *(Corresponding author: Yan Li.)*

Jinliang Liu and Zihao Liu are with the School of Computer Science, Nanjing University of Information Science and Technology, Nanjing 210044, China (e-mail: liujinliang@vip.163.com; liuzihao202506@163.com).

Yan Li is with the School of Computer and Artificial Intelligence, Nanjing University of Finance and Economics, Nanjing 210023, China (e-mail: ylnjue@163.com).

Engang Tian is with the School of Optical-Electrical and Computer Engineering, University of Shanghai for Science and Technology, Shanghai 200093, China (e-mail: tianengang@163.com).

Chen Peng is with the School of Mechatronic Engineering and Automation, Department of Automation, Shanghai University, Shanghai 200444, China (e-mail: c.peng@shu.edu.cn).

Digital Object Identifier 10.1109/TVT.2026.3651837

By integrating psychical components and onboard communication systems, USVs can be driven by dedicated control algorithms to execute increasingly complex tasks with minimal human involvement [3], [4]. As a result, they hold significant potential for applications such as marine resource exploration, environmental monitoring, maritime search and rescue, and water quality sampling [5], [6], [7], [8]. It is now widely recognized that the formation control is a crucial prerequisite for mission success [9], [10]. Thus, various formation control methods have been proposed in the literature. In [11], based on designing appropriate performance index function, an optimal control strategy is proposed to achieve prescribed performance-based formation control of USVs. In [12], a fuzzy logic system is developed to reconstruct the unmodeled dynamics and external disturbances of the controlled USVs, so as to cope with the formation control problem of multiple USVs with sensor faults. In [13], the authors explore the adaptive formation control problem of underactuated USVs by employing an updated first-order filter and adaptive estimation. However, the objectives of USVs may conflict during the collaborative execution of specific tasks [14], and thus the research interest in using game theory to depict the interactions among USVs is growing.

Game theory has been extensively applied to solve cooperative and competitive problems in diverse applications [15]. In particular, noncooperative game has become a powerful tool for analyzing situations where players act independently to maximize their individual objectives by taking the influence of other players into account [16]. Focusing on the formation control of USVs, noncooperative game models have been employed to mitigate actuator faults, uncertainties, and external disturbances [17], [18]. Furthermore, a fully distributed estimation strategy based on this theory is presented in [19] to ensure formation control between the target and the followers. The mentioned studies assume that the data exchange between USVs are secure without any information leakage, however, in practical USV missions, the communication channels are likely to be compromised by eavesdropping attacks, which will lead to the instability in formation control of USVs.

To effectively resolve the problem of information being easily intercepted during transmission, privacy protection mechanism has become a prominent research focus [20]. The basic operation of privacy protection is to transform critical data into an alternative form using encryption algorithms, and then the original data can only be recovered by the holders of the correct decryption key [21], [22]. Related research has advanced across multiple fields [23]. In [24], the authors employ a hybrid encryption approach which combines asymmetric and symmetric encryption algorithms, and apply it for the first time to multi-agent systems for enhancing communication security. In [25], a privacy-preserving distributed algorithm based on partially homomorphic encryption is designed to protect sensitive information of power system states. Nevertheless, due to the exposed propagation characteristics of maritime wireless signals, communication signals between USVs and their neighbors are highly susceptible to interception by attackers. Traditional encryption methods may not be suitable in this context, as maritime interference can cause synchronization failures in encryption keys, which will compromise the reliability of the communication. In addition, more complex encryption techniques, such as homomorphic encryption, are computationally demanding and may introduce significant delays, which could disrupt the formation balance. This motivates our work to develop a cost-efficient privacy-protected formation control strategy for USVs to mitigate the impact of eavesdropping attacks.

Besides the privacy-preserving issue, the difficulty in acquiring accurate system parameters also presents a great challenge to the formation control of USVs. Notably, neural networks have emerged as a powerful solution to overcome the challenge due to their universal approximation capabilities and adaptive learning properties [26]. In [27], a prescribed performance control strategy based on neural networks is introduced, which enables efficient trajectory tracking control for USVs despite model uncertainties and environmental disturbances. In [28], a radial basis function neural network (RBFNN) is employed to approximate the unknown dynamics of USVs, which is followed by the development of a novel adaptive tracking control scheme. Although these studies offer valuable approaches for formation control of USVs in diverse scenarios [29], the issue of slow convergence of neural networks in complex environments remains unaddressed. Unlike traditional neural networks, echo state network (ESN) trains only output weights, significantly enhancing efficiency. Therefore, this work adopts the ESN to address unknown USV dynamics.

On the basis of the above observations, this paper dedicates to develop a distributed control method within noncooperative game framework for formation control of USVs with uncertain parameters and eavesdropping attacks. The major contributions of the work can be concluded as follows.

1) *Designing privacy-protected estimator under eavesdropping attacks:* A privacy-protected estimator is devised for each USV to estimate the actions of other USVs, and then facilitating the formation control of USVs, where a twin-network structure is incorporated to guarantee the confidentiality of the data throughout the process.
2) *Proposing novel neural predictor for unknown system dynamics:* To effectively approximate the dynamics of USVs with unknown parameters, a neural predictor based on an accelerated learning-boosted ESN (ALESN) is designed, in which the ALESN can significantly enhance the convergence speed and prediction accuracy by integrating advanced learning techniques.
3) *Developing distributed formation control strategy based on Nash equilibrium seeking:* A noncooperation game model is firstly established to capture the interactions among USVs. Then, a distributed formation control method for the USVs with the designed estimator and predictor is proposed by seeking the Nash equilibrium in the constructed game.

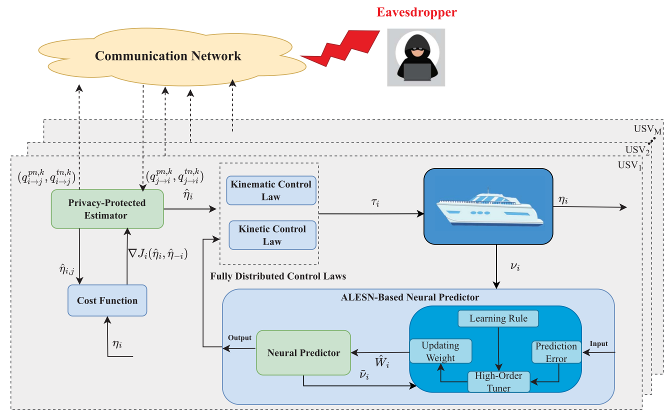


Fig. 1. The control frame of the USVs.

The remainder of this paper is organized as follows. Section II presents the description of the USVs and noncooperative game model, along with a detailed problem formulation. The design and analysis of the envisioned distributed formation control method are provided in Section III and Section IV, respectively. Simulation results are discussed in Section V and the conclusion of the paper is given in Section VI.

## II. Problem Formulation

In this section, the system dynamics and communication topology of USVs are firstly introduced. Then, the investigated problem under the noncooperation game framework is specifically formulated.

### A. Description of the USVs

The considered system is assumed to be composed by $M$ homogeneous USVs as shown in Fig. 1. The $M$ USVs exchange information through a communication network, and the interaction topology is described by a directed graph $G = \{\mathcal{P}, E\}$, where $\mathcal{P} = \{1, \ldots, M\}$ denotes the set of $M$ USVs, and $E \subseteq \mathcal{P} \times \mathcal{P}$ represents the set of directed edges. An edge $< i, j > \in E$ indicates that USV$_j$ can receive information from USV$_i$. The corresponding adjacency matrix of $G$ is denoted as $V = [\rho_{ij}] \in \mathbb{R}^{M\times M}$, where $\rho_{ij} = 1$ if $< i, j > \in E$ and $\rho_{ij} = 0$ otherwise. The Laplacian matrix of $G$ is defined as $\mathcal{L} = [l_{ij}] \in \mathbb{R}^{M\times M}$, where $l_{ij} = -\rho_{ij}$ and $l_{ii} = \sum_{j=1}^{M} \rho_{ij}$.

The kinematics and kinetics of each USV$_i$ $(1 \leq i \leq M)$ is depicted as

$$\begin{cases} \dot{\eta}_i = R(\psi_i)\nu_i \\ M_i\dot{\nu}_i = \tau_i + f_i(\nu_i) + \omega_i \end{cases} \tag{1}$$

where $\eta_i = [x_i, y_i, \psi_i]^T \in \mathbb{R}^3$ with $x_i$, $y_i$ being the two-dimensional position and $\psi_i$ represent the heading angle measured in the earth-fixed coordinate system; The vector $\nu_i = [u_i, v_i, r_i]^T \in \mathbb{R}^3$ denotes the surge, sway, and yaw velocities; $M_i \in \mathbb{R}^{3\times 3}$ is the inertia matrix; $f_i(\nu_i) \in \mathbb{R}^3$ represents an unknown nonlinear term (e.g., Coriolis and centripetal forces, hydrodynamics); $\tau_i \in \mathbb{R}^3$ is the control input vector and $\omega_i \in \mathbb{R}^3$ is the uncertain and bounded environmental disturbance; $R(\psi_i) \in \mathbb{R}^{3\times 3}$ represents the rotation matrix with the following form

$$\begin{bmatrix} \cos(\psi_i) & -\sin(\psi_i) & 0 \\ \sin(\psi_i) & \cos(\psi_i) & 0 \\ 0 & 0 & 1 \end{bmatrix}.$$

### *B. Noncooperation Game Model*

In this study, a noncooperative game is constructed to depict the interactions among the considered $M$ USVs, and the specific game model is described as $\mathcal{G} = \{\mathcal{P}, \{\Theta_i\}_{i\in\mathcal{P}}, \{J_i(\eta)\}_{i\in\mathcal{P}}\}$, where $\mathcal{P}$ is the set of players, i.e., the $M$ USVs; $\Theta_i = \{\eta_i | \eta_i \in [\eta_{i,\min}, \eta_{i,\max}]\}$ represents the set of possible actions of USV$_i$ ($\eta_i$ is viewed as the action of USV$_i$ in the game); $J_i(\eta) : \Theta_1 \times \ldots \times \Theta_M \to \mathbb{R}$ is the cost function in terms of the action vector $\eta = [\eta_1, \ldots, \eta_M] \in \mathbb{R}^{3M}$. Within the game framework, the overall formation control objective is to ensure that USVs can maintain the desired formation pattern during operation; in addition, some of the USVs have their individual aims that maintain a specific displacement relative to the reference trajectory $\eta_0$. The specific formulations of the two kinds of objectives are introduced as below.

1) To achieve the overall formation control objective, it is necessary to minimize the formation error with respect to neighbors for each USV, which can be formulated as $\min_{i\in\mathcal{P}} \sum_{j=1}^{M} \rho_{ij} \|\eta_i - \eta_j - d_{ij}\|^2$, where $d_{ij}$ is the desired formation displacement between USV$_i$ and USV$_j$.

2) To achieve the described individual objective, it is required to minimize the tracking error with respect to the reference target for each corresponding USV, which can be formulated as $\min_{i\in\mathcal{P}_0} \|\eta_i - \eta_0 - d_{i0}\|^2$, where $\mathcal{P}_0$ indicates the set of USVs with individual objectives, and $d_{i0}$ is the desired displacement between USV$_i$ and the reference target with trajectory $\eta_0$.

By integrating the objectives, the cost function in the game is specifically defined as

$$J_i(\eta_i, \eta_{-i}) = \sum_{j=1}^{M} \frac{\rho_{ij}}{2} \|\eta_i - \eta_{i,j} - d_{ij}\|^2 + \frac{\zeta_i}{2} \|\eta_i - \eta_0 - d_{i0}\|^2 \tag{2}$$

where $\eta_{i,j} \in \mathbb{R}^3$ represents the action of USV$_j$ observed by USV$_i$ and $\eta_{-i} = [\eta_{i,1}^T, \ldots, \eta_{i,i-1}^T, \eta_{i,i+1}^T, \ldots, \eta_{i,M}^T]^T \in \mathbb{R}^{3(M-1)}$; $\zeta_i \in \{0, 1\}$ is the tracking weight of USV$_i$, $\zeta_i = 1$ if $i \in \mathcal{P}_0$ and vice versa. Then, it follows from (2) that

$$\nabla J_i(\eta_i, \eta_{-i}) = \sum_{j=1}^{M} \rho_{ij}(\eta_i - \eta_{i,j} - d_{ij}) + \zeta_i(\eta_i - \eta_0 - d_{i0}). \tag{3}$$

*Remark 1:* The first two terms in (2) correspond to the overall formation and individual control objectives, respectively. Notably, both are assigned equal weights of $\frac{1}{2}$, implying equal contributions to the total cost, though these can be adjusted according to practical needs. Furthermore, the fact that $d_{i0} - d_{j0}$ may not equal $d_{ij}$ indicates a potential conflict between these two objectives.

## III. Nash Equilibrium-Based Control Method

Within the noncooperative game framework, we firstly design a privacy-protected estimator that protects the exchanged information using a twin-network structure. Then, an ALESN-based neural predictor is proposed to approximate the unknown dynamics of USVs. Finally, a distributed formation control method composed by two control laws is developed via employing a Nash equilibrium seeking strategy.

### *A. The Twin-Network-Based Privacy-Protected Estimator*

In this study, it is assumed that each USV can not directly obtain the actions of other USVs. Thus, an action estimator is designed by using estimation signals from its neighbors. Moreover, due to the unshielded propagation characteristics of maritime wireless signals and the high computational burden of traditional encryption methods, USV formations require a lightweight and efficient privacy mechanism to mitigate the risk of information leakage caused by eavesdroppers in the communication network. Towards this end, a privacy-protected mechanism based on a twin-network structure is implemented to ensure data security [30]. The structure means that the estimated values of each USV are derived from both the physical layer and twin layer estimations. Specifically, for USV$_j$ ($1 \le j \le M$), $\hat{\eta}_{j,k} \in \mathbb{R}^3$ ($1 \le k \le M$) denotes its estimation for $\eta_k$ at the physical layer, meanwhile, a virtual value $h_k^j \in \mathbb{R}^3$ is generated accordingly at the twin layer ($\hat{\eta}_{j,j}$ is referred to as $\hat{\eta}_j$ and it is assumed that $\hat{\eta}_j = \eta_j$ and $h_j^j = h_j$). Then, instead of sending $\hat{\eta}_{j,k}$ and $h_k^j$ to its neighbors, e.g., USV$_i$, USV$_j$ will transmit the following masked information $q_{j\to i}^{pn,k}$ and $q_{j\to i}^{tn,k}$ over the network.

$$\begin{cases} q_{j\to i}^{pn,k} = \hat{\eta}_{j,k} - \Upsilon h_k^j + p_{j,i}^{pn} \\ q_{j\to i}^{tn,k} = \beta h_k^j + \Upsilon \hat{\eta}_{j,k} + p_{j,i}^{tn} \end{cases} \tag{4}$$

where $\Upsilon$ and $\beta$ are positive scalar coupling gains designed offline before deploying; the signals $p_{j,i}^{pn}$ and $p_{j,i}^{tn}$ are private, bounded masking signals known only to the sender USV$_j$.

Based on receiving the masked information from neighbors, the estimator for each USV$_i$ is designed as

$$\begin{cases} \dot{\hat{\eta}}_{i,k} = -(\hat{\eta}_{i,k} - \Upsilon h_k^i) + \sum_{j=1}^{M} \rho_{ji} q_{j\to i}^{pn,k} \\ \dot{h}_k^i = -(\Upsilon \hat{\eta}_{i,k} + \beta h_k^i) + \sum_{j=1}^{M} \rho_{ji} q_{j\to i}^{tn,k}. \end{cases} \tag{5}$$

According to the estimated actions of USVs, the cost function (2) is updated as

$$J_i(\hat{\eta}_i, \hat{\eta}_{-i}) = \sum_{j=1}^{M} \frac{\rho_{ij}}{2} \|\hat{\eta}_i - \hat{\eta}_{i,j} - d_{ij}\|^2 + \frac{\zeta_i}{2} \|\hat{\eta}_i - \eta_0 - d_{i0}\|^2 \tag{6}$$

where $\hat{\eta}_{-i} = \left[\hat{\eta}_{i,1}^T, \ldots, \hat{\eta}_{i,i-1}^T, \hat{\eta}_{i,i+1}^T, \ldots, \hat{\eta}_{i,M}^T\right]^T \in \mathbb{R}^{3(M-1)}$. It follows from (6) that

$$\nabla J_i(\hat{\eta}_i, \hat{\eta}_{-i}) = \sum_{j=1}^{M} \rho_{ij}(\hat{\eta}_i - \hat{\eta}_{i,j} - d_{ij}) + \zeta_i(\hat{\eta}_i - \eta_0 - d_{i0}). \tag{7}$$

*Remark 2:* Given that eavesdropping attacks, which are inherently difficult to model mathematically, are considered in this study, the active privacy-protected mechanism based on the twin-network structure is employed to mitigate the leakage of sensitive information. In the mechanism, the virtual value $h_k^j$ has no practical meaning. With this mechanism, external eavesdroppers who intercept the transmitted signals $q_{j\to i}^{pn,k}$ and $q_{j\to i}^{tn,k}$ still can not uniquely determine the meaningful estimated value $\hat{\eta}_{j,k}$. The reason is that the two equations given in (4) are driven by multiple variables, and then it is computationally impossible to accurately recover the confidential information without the knowledge of these parameters. Moreover, compared to traditional encryption methods, the twin-network framework effectively reduces computational overhead while ensuring privacy protection.

### B. The ALESN-Based Neural Predictor

In practice, USVs are generally subject to various external uncertainties and exhibit complex nonlinear characteristics. Therefore, this study propose an ALESN-based neural predictor to forecast the kinetics of USVs. To be specific, the kinematic equation of USV$_i$ is firstly rewritten as

$$\dot{\nu}_i = F_i(\nu_i) + M_i^{-1}\tau_i \tag{8}$$

where $F_i(\nu_i) = M_i^{-1}\big(f_i(\nu_i) + \omega_i\big)$. As shown, $F_i(\nu_i)$ consists of the unknown nonlinear term $f_i(\nu_i)$ and positional disturbance $\omega_i$, so an ESN introduced in [31] is adopted to approximate it as follows.

$$F_i(\cdot) = W_i^{*T} X_i + \varepsilon_i \tag{9}$$

where $W_i^* \in \mathbb{R}^{M\times 3}$ is the ideal output weight matrix of the ESN; $X_i \in \mathbb{R}^M$ is the reservoir state; $\varepsilon_i \in \mathbb{R}^3$ is the approximation error, satisfying $\|\varepsilon_i\| \le \varepsilon_i^*$ with $\varepsilon_i^* \in \mathbb{R}^+$.

Given the difficulty in acquiring the exact value of $W_i^*$, an adaptive law based on accelerated learning is proposed to estimate it with improved convergence speed.

$$\begin{cases} \dot{Z}_i = -b_i\xi_i X_i \varphi_i^T \\ \dot{\hat{W}}_i = -c_i(\hat{W}_i - Z_i) \end{cases} \tag{10}$$

where $\hat{W}_i \in \mathbb{R}^{M\times 3}$ is the estimation of $W_i^*$; $\xi_i = \frac{1}{1+\|X_i\|^2}$ is a scaling factor; $b_i$ and $c_i$ are positive tuning parameters; $\varphi_i$ is an auxiliary variable which will be explained shortly. Consequently, the ALESN-based neural predictor for the kinetics is constructed as below.

$$\dot{\hat{\nu}}_i = M_i^{-1}\tau_i + \hat{W}_i^T X_i - K_{i,1}\tilde{\nu}_i \tag{11}$$

where $\hat{\nu}_i \in \mathbb{R}^3$ is the estimation of $\nu_i$; $K_{i,1} = \mathrm{diag}\{k_{u,i}, k_{v,i}, k_{r,i}\} \in \mathbb{R}^{3\times 3}$ with $k_{u,i}$, $k_{v,i}$, and $k_{r,i}$ being positive control gains; $\tilde{\nu}_i = \hat{\nu}_i - \nu_i$ denotes the prediction error. Furthermore, according to (8), (9) and (11), it has

$$\dot{\tilde{\nu}}_i = \tilde{W}_i^T X_i - K_{i,1}\tilde{\nu}_i - \varepsilon_i \tag{12}$$

where $\tilde{W}_i = \hat{W}_i - W_i^*$, and $\varphi_i$ in (10) is thereby defined as $\varphi_i = \dot{\tilde{\nu}}_i + K_{i,1}\tilde{\nu}_i$.

*Remark 3:* ESN eliminates the input training process via a reservoir structure with fixed input weights. Compared to fuzzy systems [32] and RBFNN [33], ESN requires fewer tunable parameters, which reduces complexity and enhances efficiency. Moreover, the accelerated learning technique demonstrates superior convergence speed compared to traditional gradient descent-based methods [34], [35]. The accelerated learning introduces a two-stage update, i.e., the intermediate state $\dot{Z}_i = -b_i\xi_i X_i\varphi_i^T$, while the weight estimate $\hat{W}_i$ tracks $Z_i$ via $c_i$. This decouples $\hat{W}_i$ from instantaneous nonlinear dynamics so as to oscillations and accelerating convergence. By incorporating the derivative term $\varphi_i$, $Z_i$ can pre-adjust the weight update direction, then reduce lag and improve dynamic prediction. The normalization term $\xi_i$ further limits large updates, thereby enhancing numerical stability.

### C. The Formation Control Method Based on Nash Equilibrium Seeking

In this subsection, the distributed formation controller is designed for each USV by using a Nash equilibrium seeking approach. For the established noncooperative game, a strategy profile $\eta^* = (\eta_1^*, \ldots, \eta_M^*)$ is called a Nash equilibrium if there is no USV can decrease its cost by unilaterally changing its own action. In other words, for $\forall\ i \in \mathcal{P}$ and $\forall\ \eta_i \in \Theta_i$, it has $J_i(\eta_i^*, \eta_{-i}^*) \le J_i(\eta_i, \eta_{-i}^*)$, where $\eta_i^* \in \mathbb{R}^3$ denotes the optimal game solution of USV$_i$ and $\eta_{-i}^* = [{\eta_1^*}^T, \ldots, {\eta_{i-1}^*}^T, {\eta_{i+1}^*}^T, \ldots, {\eta_M^*}^T]^T \in \mathbb{R}^{3(M-1)}$. A Nash equilibrium exists in the game $\mathcal{G}$ if for $\forall\ i \in \mathcal{P}$, $\Theta_i$ is a nonempty, convex, and compact subset of $\mathbb{R}$, and $J_i(\eta_i, \eta_{-i})$ is convex and continuously differentiable [36]. According to the description on $\mathcal{G}$, it follows that a Nash equilibrium solution must exist. Then, a Nash equilibrium seeking strategy $\dot{\eta}_i^* = \delta_i g(\hat{\eta}_i)$ is used to obtain the optimal game solution of USV$_i$, where $\delta_i \in \mathbb{R}^{3\times 3}$ is a given gain matrix; $g(\hat{\eta}_i) = \nabla J_i(\hat{\eta}_i, \hat{\eta}_{-i})$ which has been derived in (7). It is evident that the gradient is Lipschitz continuous.

Based on the Nash equilibrium seeking strategy and the designed estimator and predictor, the formation control method is subsequently devised in two steps.

*Step 1:* The kinematic error is defined as $e_{i,1} = R^T(\psi_i)(\eta_i - \eta_i^*)$. Taking the time derivative of $e_{i,1}$, it can be obtained that

$$\dot{e}_{i,1} = \dot{R}^T(\psi_i)(\eta_i - \eta_i^*) + \nu_i - R^T(\psi_i)\dot{\eta}_i^*. \tag{13}$$

Based on (13), the kinematic control law is formulated as follows

$$\alpha_i = -K_{i,2}e_{i,1} - \dot{R}^T(\psi_i)(\eta_i - \eta_i^*) + R^T(\psi_i)\dot{\eta}_i^* \tag{14}$$

where $K_{i,2} = \mathrm{diag}\{k_{x,i}, k_{y,i}, k_{\psi,i}\} \in \mathbb{R}^{3\times 3}$ with $k_{x,i}$, $k_{y,i}$, and $k_{\psi,i}$ being positive control gains. Additionally, for avoiding the complex derivation of $\alpha_i$, a linear second-order filter is introduced as follows.

$$\begin{cases} \dot{\alpha}_{f,i} = a_{fd,i} \\ \dot{a}_{fd,i} = -2\zeta_i \omega_{n,i}\, a_{fd,i} - \omega_{n,i}^2 \left(a_{f,i} - \alpha_i\right) \end{cases} \tag{15}$$

where $\alpha_{f,i} \in \mathbb{R}^3$ and $\alpha_{fd,i} \in \mathbb{R}^3$ are the estimations of $\alpha_i$ and $\dot{\alpha}_i$, respectively; $\omega_{n,i} > 0$ is the natural frequency of the filter; $\zeta_i > 0$ is the damping ratio.

*Step 2:* The prediction kinetic error is defined as $\hat{e}_{i,2} = \hat{\nu}_i - \alpha_{f,i}$, and taking the time derivative of $\hat{e}_{i,2}$, it yields that

$$\dot{\hat{e}}_{i,2} = M_i^{-1}\tau_i + \hat{W}_i^T X_i - K_{i,1}\tilde{\nu}_i - \alpha_{fd,i} \tag{16}$$

Based on (16), the following kinetic control law is developed.

$$\tau_i = M_i\Big(-K_{i,1}e_{i,2} - \hat{W}_i^T X_i + \alpha_{fd,i} - e_{i,1}\Big) \tag{17}$$

where $e_{i,2} = \nu_i - \alpha_{f,i}$. Finally, by referring to (13), (14), (16) and (17), a dynamic error system can be established as below.

$$\begin{cases} \dot{e}_{i,1} = -K_{i,2}e_{i,1} + \hat{e}_{i,2} - \tilde{\nu}_i + \tilde{a}_i \\ \dot{\hat{e}}_{i,2} = -K_{i,1}\hat{e}_{i,2} - e_{i,1} \end{cases} \tag{18}$$

where $\tilde{a}_i = a_{f,i} - a_i$.

## IV. Performance Analysis

In this section, the effectiveness of the presented estimation method is firstly demonstrated in Theorem 1. Then, we show that the prediction error system (11) and dynamic error system (18) are input-to-state stable (ISS) in Theorem 2. The following assumption and lemma are stated to facilitate the subsequent analysis.

*Assumption 1:* The communication network $G$ which governs the USVs forms a strongly connected graph.

*Lemma 1 ([30]):* The matrix $\Phi_{[k]} = \begin{bmatrix} 1 & -\Upsilon \\ \Upsilon & \beta \end{bmatrix} \otimes \mathscr{A}_{[k]}$ is Hurwitz if Assumption 1 is satisfied and the positive scalar gains $\Upsilon$, $\beta$ are selected such that

$$\beta - 1 < 2\Upsilon < \sqrt{\frac{(\beta+1)^2 + \theta^2(\beta-1)^2}{\theta^2}} \tag{19}$$

where $\theta = \max_i \frac{|\Im(\lambda_i(\mathscr{A}_{[k]}))|}{|\Re(\lambda_i(\mathscr{A}_{[k]}))|}$; the matrix $\mathscr{A}_{[k]} \in \mathbb{R}^{(M-1)\times(M-1)}$ is obtained from the matrix $\mathscr{A} \in \mathbb{R}^{M\times M}$ by removing the $k$-th row and $k$-th column, and $\mathscr{A}$ is defined as

$$\mathscr{A} = \begin{bmatrix} -\sum_{j=1}^M \rho_{j1} & \rho_{21} & \cdots & \rho_{M1} \\ \rho_{12} & -\sum_{j=1}^M \rho_{j2} & \cdots & \rho_{M2} \\ \vdots & \vdots & \ddots & \vdots \\ \rho_{1M} & \rho_{2M} & \cdots & -\sum_{j=1}^M \rho_{jM} \end{bmatrix}.$$

*Theorem 1:* Under Assumption 1, the devised estimator (5) can effectively estimate the actions of USVs if sufficiently large gains $\Upsilon$ and $\beta$, which satisfy (19), are chosen.

*Proof:* To simplify the proof, we treat the relevant three-dimensional parameters as one-dimensional. The derived results can be easily extended to the considered three-dimensional scenario by using the Kronecker product.

Let $\overline{\eta}_k = [\hat{\eta}_{1,k}, \ldots, \hat{\eta}_{k-1,k}, \hat{\eta}_{k+1,k}, \ldots, \hat{\eta}_{M,k}]^T \in \mathbb{R}^{M-1}$ and $\overline{h}_k = [h_k^1, \ldots, h_k^{k-1}, h_k^{k+1}, \ldots, h_k^M]^T \in \mathbb{R}^{M-1}$, then the compact form of the estimator dynamics can be written as

$$\begin{cases} \dot{\overline{\eta}}_k = \mathscr{A}_{[k]}\overline{\eta}_k + \mathscr{B}_{[k]}\eta_k - \Upsilon\mathscr{A}_{[k]}\overline{h}_k - \Upsilon\mathscr{B}_{[k]}h_k + \boldsymbol{\delta}_k^{pn} \\ \dot{\overline{h}}_k = \beta\mathscr{A}_{[k]}\overline{h}_k + \Upsilon\mathscr{A}_{[k]}\overline{\eta}_k + \Upsilon\mathscr{B}_{[k]}\eta_k + \beta\mathscr{B}_{[k]}h_k + \boldsymbol{\delta}_k^{tn} \end{cases} \tag{20}$$

where $\boldsymbol{\delta}_k^{pn} = [\delta_1^{pn}, \ldots, \delta_{k-1}^{pn}, \delta_{k+1}^{pn}, \ldots, \delta_M^{pn}]^T$ and $\boldsymbol{\delta}_k^{tn} = [\delta_1^{tn}, \ldots, \delta_{k-1}^{tn}, \delta_{k+1}^{tn}, \ldots, \delta_M^{tn}]^T$ with $\delta_i^{pn} = \sum_{j=1}^M \rho_{ji}p_{j,i}^{pn}$ and $\delta_i^{tn} = \sum_{j=1}^M \rho_{ji}p_{j,i}^{tn}$; the vector $\mathscr{B}_{[k]} \in \mathbb{R}^{M-1}$ is obtained from $\mathscr{B}_k = [\rho_{k1}, \ldots, \rho_{kM}]^T$ by removing the $k$-th element. Under Assumption 1, it is known hat the matrix $\mathscr{A}_{[k]}$ is Hurwitz [37], and it has $\mathscr{A}_{[k]}\mathbf{1}_{M-1} = -\mathscr{B}_{[k]}$.

Defining the estimator error vectors as

$$\begin{cases} \mathbf{e}_{k,\eta}^{pn} = \overline{\eta}_k - \mathbf{1}_{M-1}\eta_k \\ \mathbf{e}_{k,h}^{tn} = \overline{h}_k - \mathbf{1}_{M-1}h_k. \end{cases} \tag{21}$$

Taking the time derivative of $\mathbf{e}_{k,\eta}^{pn}$, it yields that

$$\begin{aligned} \dot{\mathbf{e}}_{k,\eta}^{pn} &= \mathscr{A}_{[k]}\mathbf{e}_{k,\eta}^{pn} + (\mathscr{A}_{[k]}\mathbf{1}_{M-1} + \mathscr{B}_{[k]})\eta_k - \mathbf{1}_{M-1}\dot{\eta}_k \\ &\quad - \Upsilon\mathscr{A}_{[k]}\mathbf{e}_{k,h}^{tn} + \boldsymbol{\delta}_k^{pn} - \Upsilon(\mathscr{A}_{[k]}\mathbf{1}_{M-1} + \mathscr{B}_{[k]})h_k \\ &= \mathscr{A}_{[k]}\mathbf{e}_{k,\eta}^{pn} - \Upsilon\mathscr{A}_{[k]}\mathbf{e}_{k,h}^{tn} + \boldsymbol{\delta}_k^{pn} - \mathbf{1}_{M-1}\dot{\eta}_k. \end{aligned} \tag{22}$$

Similarly, it can be calculated that $\dot{\mathbf{e}}_{k,h}^{tn} = \beta\mathscr{A}_{[k]}\mathbf{e}_{k,h}^{tn} + \Upsilon\mathscr{A}_{[k]}\mathbf{e}_{k,\eta}^{pn} + \boldsymbol{\delta}_k^{tn} - \mathbf{1}_{M-1}\dot{h}_k$. The error dynamics $\dot{\mathbf{e}}_{k,\eta}^{pn}$ and $\dot{\mathbf{e}}_{k,h}^{tn}$ can be combined in a compact form as

$$\begin{bmatrix} \dot{\mathbf{e}}_{k,\eta}^{pn} \\ \dot{\mathbf{e}}_{k,h}^{tn} \end{bmatrix} = \Phi_{[k]} \begin{bmatrix} \mathbf{e}_{k,\eta}^{pn} \\ \mathbf{e}_{k,h}^{tn} \end{bmatrix} + \begin{bmatrix} \boldsymbol{\delta}_k^{pn} - \mathbf{1}_{M-1}\dot{\eta}_k \\ \boldsymbol{\delta}_k^{tn} - \mathbf{1}_{M-1}\dot{h}_k \end{bmatrix}. \tag{23}$$

Let $\mathbf{e}_k = [\mathbf{e}_{k,\eta}^{pn}, \mathbf{e}_{k,h}^{tn}]^T$ and $\boldsymbol{\delta}_k = [\boldsymbol{\delta}_k^{pn} - \mathbf{1}_{M-1}\dot{\eta}_k, \boldsymbol{\delta}_k^{tn} - \mathbf{1}_{M-1}\dot{h}_k]^T$, then (23) can be updated as

$$\dot{\mathbf{e}}_k = \Phi_{[k]}\mathbf{e}_k + \boldsymbol{\delta}_k. \tag{24}$$

The solution to (24) can be given as

$$\mathbf{e}_k = \exp(\Phi_{[k]}t)\mathbf{e}_k(0) + \int_0^t \exp(\Phi_{[k]}(t-\tau))\boldsymbol{\delta}_k(\tau)d\tau. \tag{25}$$

Then, it can be computed that

$$\begin{aligned} \lim_{t\to\infty} \|\mathbf{e}_k\| &= \lim_{t\to\infty} \|\exp(\Phi_{[k]}t)\mathbf{e}_k(0) + \\ &\qquad \int_0^t \exp(\Phi_{[k]}(t-\tau))\boldsymbol{\delta}_k(\tau)d\tau\|. \end{aligned} \tag{26}$$

By applying Cauchy-Schwartz inequality and noting from Lemma 1 that $\Phi_{[k]}$ is Hurwitz with satisfied conditions, it has $\lim_{t\to\infty}\|\mathbf{e}_k\| \le \lim_{t\to\infty}\|\int_0^t \exp(\Phi_{[k]}(t-\tau))\boldsymbol{\delta}_k(\tau)d\tau\|$. Given that $\dot{\eta}_k$, $\dot{h}_k$, $p_{j,i}^{pn}$ and $p_{j,i}^{tn}$ are all uniformly bounded, the vector $\boldsymbol{\delta}_k$ is also uniformly bounded. So there exists a constant vector $\overline{\boldsymbol{\delta}}$ such that $\|\int_0^t \exp(\Phi_{[k]}(t-\tau))\boldsymbol{\delta}_k(\tau)d\tau\| \le \|\int_0^t \exp(\Phi_{[k]}(t-\tau))\overline{\boldsymbol{\delta}}d\tau\|$. Thus, one can obtain that $\lim_{t\to\infty}\|\mathbf{e}_k\| \le \lim_{t\to\infty}\|\int_0^t \exp(\Phi_{[k]}(t-\tau))\overline{\boldsymbol{\delta}}d\tau\| \le \|-\Phi_{[k]}^{-1}\overline{\boldsymbol{\delta}}\|$, where matrix $\Phi_{[k]}^{-1} = \begin{bmatrix} \phi_1^k & \phi_2^k \\ \phi_3^k & \phi_4^k \end{bmatrix}$ and $\phi_1^k, \phi_2^k, \phi_3^k, \phi_4^k$

are given by $\phi_1^k = \mathscr{A}_{[k]}^{-1} - \Upsilon^2(\beta\mathscr{A}_{[k]} + \Upsilon^2\mathscr{A}_{[k]})^{-1}$, $\phi_2^k = \Upsilon(\beta\mathscr{A}_{[k]} + \Upsilon^2\mathscr{A}_{[k]})^{-1}$, $\phi_3^k = -\Upsilon(\beta\mathscr{A}_{[k]} + \Upsilon^2\mathscr{A}_{[k]})^{-1}$, and $\phi_4^k = (\beta\mathscr{A}_{[k]} + \Upsilon^2\mathscr{A}_{[k]})^{-1}$. We can further write the $\phi_l^k$ $(1 \le l \le 4)$ as $\phi_1^k = \frac{\beta}{\Upsilon^2+\beta}\mathscr{A}_{[k]}^{-1}$, $\phi_2^k = \frac{\Upsilon}{\Upsilon^2+\beta}\mathscr{A}_{[k]}^{-1}$, $\phi_3^k = \frac{-\Upsilon}{\Upsilon^2+\beta}\mathscr{A}_{[k]}^{-1}$, and $\phi_4^k = \frac{1}{\Upsilon^2+\beta}\mathscr{A}_{[k]}^{-1}$. Consequently, the estimation error $\mathbf{e}_k$ can be driven to an arbitrarily small neighborhood of around zero by selecting appropriate gains $\Upsilon$ and $\beta$ that satisfy the condition given in (19) (it is important to emphasize that the gain parameters do not need to be excessively large, as doing so could lead to unnecessary signal redundancy and computational burden). This ensures the efficiency of the proposed distributed estimator (5).

*Theorem 2:* For the USVs formation with kinematics and kinetics described by (1), incorporating the ALESN-based neural predictor depicted by (11), and the distributed control laws outlined in (14) and (17), the error dynamics presented in (11) and (18) reveal ISS if Assumption 1 holds.

*Proof:* Firstly, the ISS of the prediction error system (11) is demonstrated. We define the following Lyapunov function.

$$V_{1,i} = \frac{1}{2}\tilde{\nu}_i^T\tilde{\nu}_i + \frac{1}{b_i}\|Z_i - W_i^*\|_F^2 + \frac{1}{b_i}\|Z_i - \hat{W}_i\|_F^2. \tag{27}$$

Taking the time derivative of $V_{1,i}$, we get

$$\begin{aligned}\dot{V}_{1,i} = {} & \tilde{\nu}_i^T(\tilde{W}_i^T X_i - K_{i,1}\tilde{\nu}_i - \varepsilon_i) \\ & + \frac{2}{b_i}\,\mathrm{tr}\Big([Z_i - \hat{W}_i + \tilde{W}_i]^T(-b_i\xi_i X_i\varphi_i^T)\Big) \\ & + \frac{2}{b_i}\,\mathrm{tr}\Big([Z_i - \hat{W}_i]^T[(-b_i\xi_i X_i\varphi_i^T) + c_i(\hat{W}_i - Z_i)]\Big).\end{aligned} \tag{28}$$

The equation can be further written as

$$\begin{aligned}\dot{V}_{1,i} = {} & \tilde{\nu}_i^T\,(e_i - K_{i,1}\tilde{\nu}_i) \\ & + \xi_i\Big\{\mathrm{tr}\Big(-2(\varphi_i + \varepsilon_i)\varphi_i^T - \frac{2c_i}{b_i\xi_i}\,\mathrm{tr}\,\big([\hat{W}_i - Z_i]^T[\hat{W}_i - Z_i]\big)\Big) \\ & - \frac{2c_i}{b_i}\|X_i\|^2\,\mathrm{tr}\Big([\hat{W}_i - Z_i]^T[\hat{W}_i - Z_i]\Big) \\ & + 4\,\mathrm{tr}\Big([\hat{W}_i - Z_i]^T X_i\varphi_i^T\Big)\Big\}.\end{aligned} \tag{29}$$

When $c_i \ge 2b_i$, it has

$$\begin{aligned}\dot{V}_{1,i} \le {} & -\lambda_{\min}(K_{i,1})\|\tilde{\nu}_i\|^2 + \|\tilde{\nu}_i\|\|\varphi_i\| - \frac{2c_i\xi_i}{b_i}\|\hat{W}_i - Z_i\|_F^2 \\ & - \xi_i\|\varphi_i\|^2 - \xi_i\,[\|e_i\| - 2\|\Theta_i - W_i\|_F\|X_i\|]^2 \\ \le {} & -\lambda_{\min}K_{i,1}\|\tilde{\nu}_i\|^2 + \|\tilde{\nu}_i\|\|\varphi_i\| - \frac{2c_i\xi_i}{b_i}\|\hat{W}_i - Z_i\|_F^2 \\ \le {} & -a_{i,1}\|G_i\|^2 + \|G_i\|\|\varphi_i\|\end{aligned} \tag{30}$$

where $a_{i,1} = \min\{\lambda_{\min}K_{i,1}, \frac{2c_i\xi_i}{b_i}\}$ and $G_i = [\|\tilde{\nu}_i\|, \|\hat{W}_i - Z_i\|_F]^T$. Noting that $\|G_i\| \ge \frac{2\|\varphi_i\|}{a_{i,1}}$, it follows that $\dot{V}_{1,i} \le -\frac{a_{i,1}}{2}\|G_i\|^2$. Then, the prediction error system is ISS. Furthermore, it has $|G_i(t)\| \le \max\{\varpi_i(\|G_i(0)\|, t) + \jmath_i(\|\varphi_i\|)\}$, where $\varpi_i(\cdot)$ and $\jmath_i(\cdot)$ represent a class $\mathcal{KL}$ function and a class $\mathcal{K}$ function, respectively.

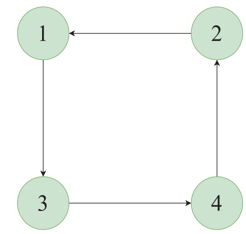


Fig. 2. The communication graph $G$.

Then, we prove the ISS of the error system depicted by (18). For this, the following Lyapunov function is constructed.

$$V_2 = \sum_{i=1}^{M}\left(\frac{1}{2}e_{i,1}^T e_{i,1} + \frac{1}{2}\hat{e}_{i,2}^T\hat{e}_{i,2}\right). \tag{31}$$

The time derivative of it is

$$\dot{V}_2 = \sum_{i=1}^{M}\left(-e_{i,1}^T K_{i,2}e_{i,1} - e_{i,1}^T\tilde{\nu}_i + e_{i,1}^T\tilde{a}_i - \hat{e}_{i,2}^T K_{i,1}\hat{e}_{i,2}\right). \tag{32}$$

Letting $Z = [E_1^T, \ldots, E_M^T]^T$ with $E_i^T = [e_{i,1}^T, \hat{e}_{i,2}^T]^T$, one can obtain

$$\begin{aligned}\dot{V}_2 \le {} & -c_z\|Z\|^2 + \|Z\|\sum_{i=1}^{M}(\|\tilde{\nu}_i\| + \|\tilde{a}_i\|) \\ \le {} & -c_z\|Z\|^2 + \|Z\|\|\overline{U}\|\end{aligned} \tag{33}$$

where $c_z = \min_{i=1}^{M}\{\lambda_{\min}(K_{i,1}), \lambda_{\min}(K_{i,2})\}$ and $\overline{U} = \mathrm{col}(U_1, \ldots, U_M)$ with $U_i = [\|\tilde{\nu}_i\|, \|\tilde{a}_i\|]$. Due to $\|\overline{U}\| \le c_z\|Z\|/2$ which implies that $\dot{V}_2 \le -c_z\|Z\|^2/2$, the error system governed by (18) is ISS, and it has $\|Z(t)\| \le \max\{\varpi_Z(\|Z(0)\|, t) + \jmath_Z(\|\overline{U}\|)\}$, where $\varpi_Z(\cdot)$ and $\jmath_Z(\cdot)$ represent a class $\mathcal{KL}$ function and a class $\mathcal{K}$ function, respectively.

## V. Simulation Results

In this section, a simulation example is provided to validate the effectiveness of the estimation-based formation control method. The example involves 4 USVs (i.e., $M = 4$) with the communication topology $G$ as shown in Fig. 2. The detailed model parameters of the USVs are set as described in [38]. The 4 USVs are required to track the reference target with the trajectory $\eta_0 = [6 + 15\sin(0.02t), 6 + 15\cos(0.02t), 0]^T$. The tuning parameters in the adaptive law (10) are given as $b_i = 1$ and $c_i = 1$. The designed gains are selected as $\mu_{i,j} = \mathrm{diag}\{1, 1, 1\}$, $\delta_i$=diag$\{0.5, 0.5, 0.5\}$, $K_{i,1} = \mathrm{diag}\{2, 2, 2\}$ and $K_{i,2} = \mathrm{diag}\{1, 1, 1\}$. The desired distance between each USV and its neighbors are set as $d_{12} = [-10, 0, 0]^T$, $d_{24} = [0, 10, 0]^T$, $d_{31} = [0, -10, 0]^T$ and $d_{43} = [10, 0, 0]^T$, which define the expected formation that we aim to achieve. The initial conditions are given as $\eta_1(0) = [5, 24, 0]^T$, $\eta_2(0) = [11, 25, 0]^T$, $\eta_3(0) = [3, 20, 0]^T$, $\eta_4(0) = [8, 19, 0]^T$and $\nu_i(0) = [0, 0, 0]^T$. For the privacy-preserving estimator, we set $\beta = 4$ and $\Upsilon = 2$. The signals $p_{j,i}^{pn}$, $p_{j,i}^{tn}$ are configured as a combination of sinusoidal

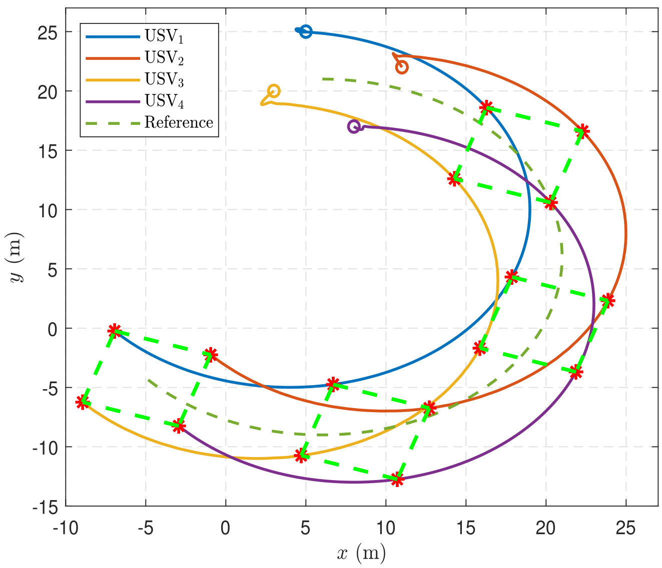


Fig. 3. The motion trajectories of 4 USVs and the reference target.

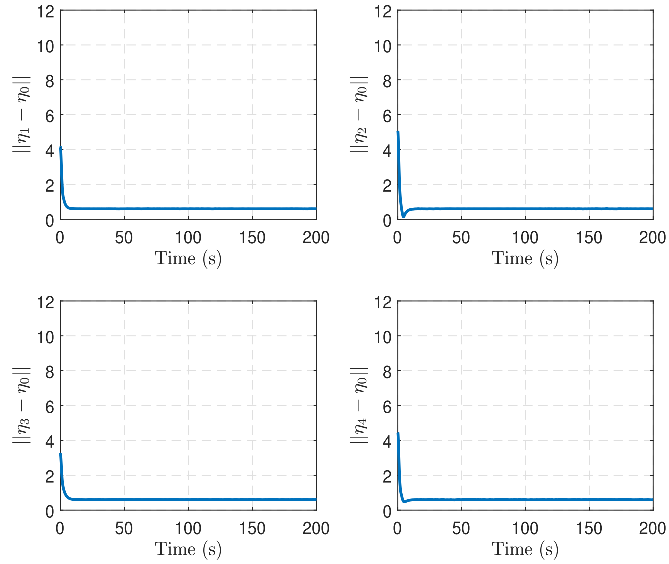


Fig. 5. Euclidean distance between USVs and the reference focusing on the tracking objective.

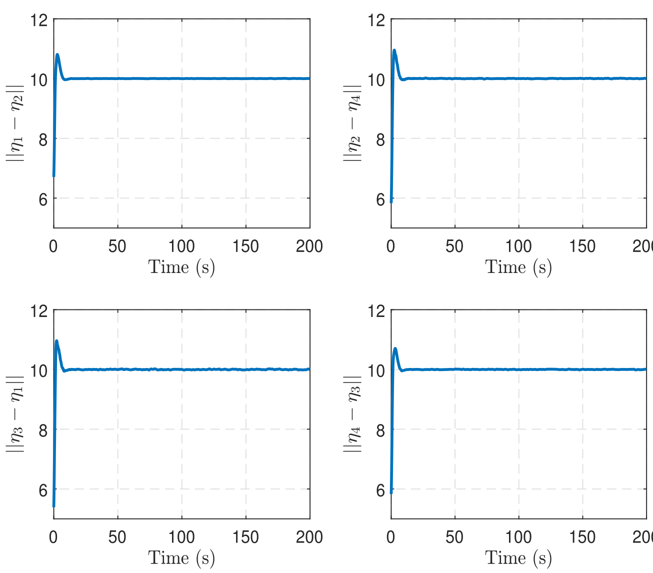


Fig. 4. Euclidean distance between connected USVs focusing on the formation objective.

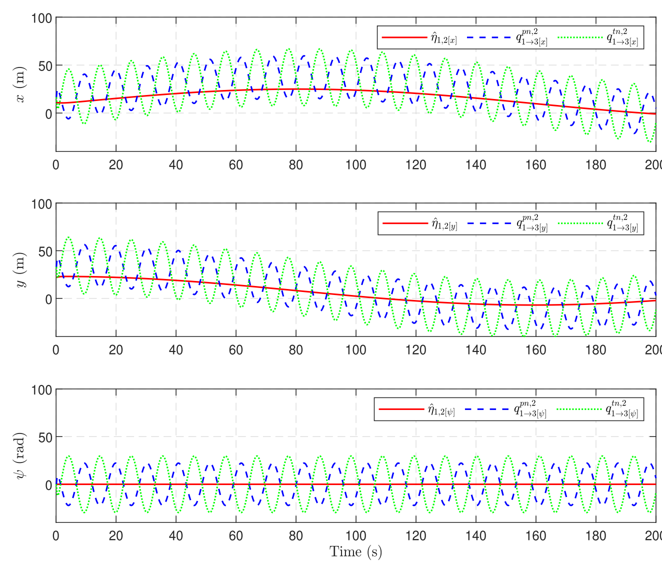


Fig. 6. $\hat{\eta}_{1,2}$ and the corresponding masked information.

signals [30]. This configuration is chosen due to the low communication and computational overhead associated with sinusoidal signal combinations. Additionally, this approach helps meet the requirements for attack resistance.

Based on the above experimental setup, the simulation results are specifically presented in Figs. 3– 12. Fig. 3 shows the motion trajectories of the 4 USVs and the reference target, where the circles on lines denote the initial positions and the green dashed quadrilaterals outline the geometric formation maintained by the 4 USVs during their motion. It can be observed that the 4 USVs maintain an efficient formation and achieve satisfactory tracking performance, which demonstrates the validity of the designed control strategy. We would like to note that there is some deviation between the actual and desired formations, as well as between each USV's trajectory and the reference trajectory. This is because the cost function of each USV represents a trade-off between the overall formation objective and the individual tracking objective. In view of this, we adjust the weights in the cost function (2) to enable that each USV focuses on one of these two objectives, then present the corresponding results in Figs. 4 and 5, respectively. Specifically, Fig. 4 reveals that the expected formation of USVs can be successfully achieved by considering only the formation objective. Meanwhile, Fig. 5 demonstrates that each USV can accurately follow the reference target by considering only the tracking objective. These results highlight the flexibility and practicality of the proposed control strategy.

Fig. 6 illustrates the efficiency of the described privacy-protected mechanism. As we mentioned before, each USV sends

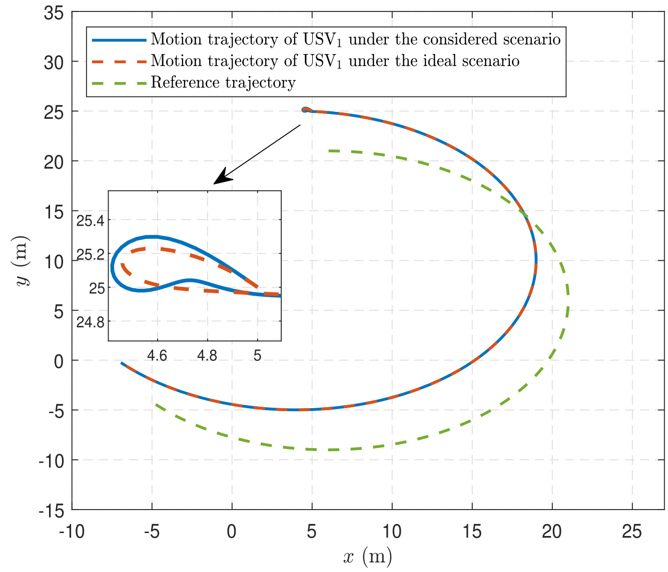


Fig. 7. The motion trajectories of USV$_1$ under different scenarios.

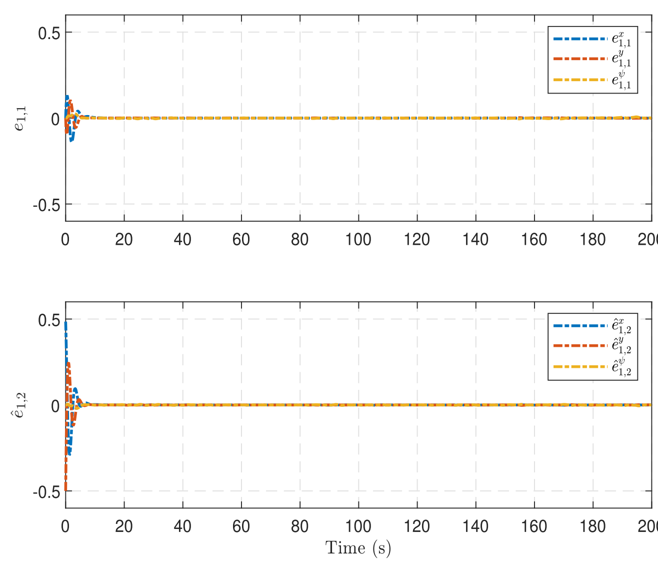


Fig. 8. Kinematic error $e_{1,1}$ and kinetic error $\hat{e}_{1,2}$.

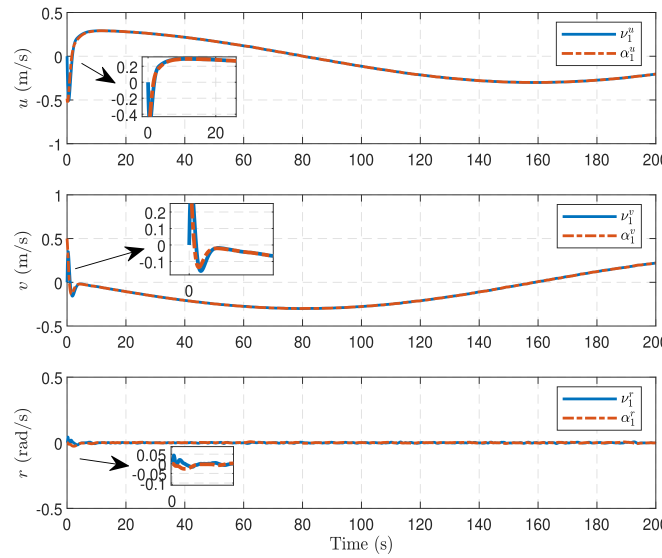


Fig. 9. The velocity $\nu_1$ and commanded velocity $\alpha_1$.

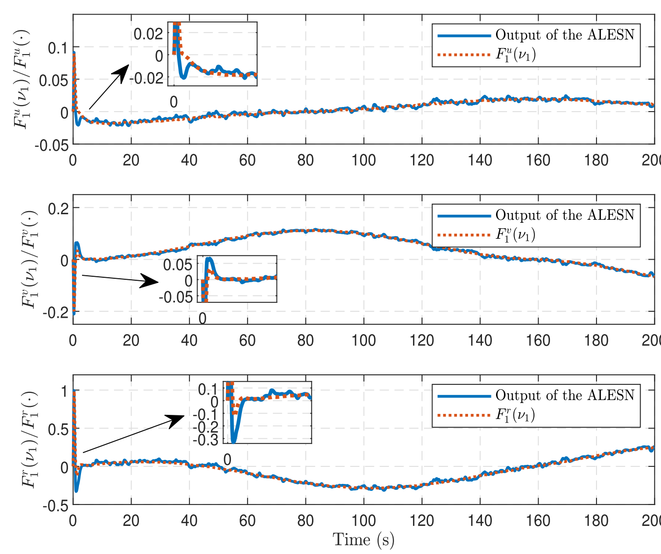


Fig. 10. Evaluating of the ALESN.

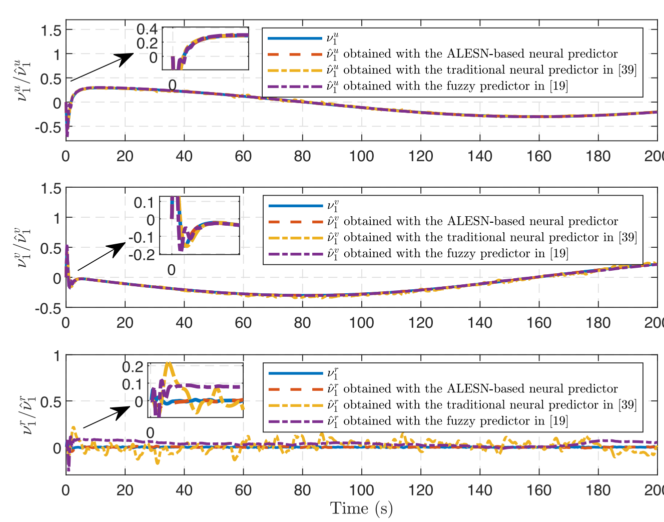


Fig. 11. The actual velocity and predicted velocity of USV$_1$.

the masked information rather than the actual local estimation signals to its neighbors under the mechanism. Thus, Fig. 6 displays the estimation generated by USV$_1$, i.e., $\hat{\eta}_{1,2}$, and the corresponding masked information transmitted to USV$_3$, i.e., $q^{pn,2}_{1\to 3}$ and $q^{tn,2}_{1\to 3}$. Here, $\hat{\eta}_{1,2[x/y/\psi]}$ ($q^{pn,2/}_{1\to 3[x/y/\psi]}q^{tn,2}_{1\to 3[x/y/\psi]}$) indicates the $1^{st}/2^{nd}/3^{rd}$ component of $\hat{\eta}_{1,2}$ ($q^{pn,2}_{1\to 3}/q^{tn,2}_{1\to 3}$), respectively. As shown, the masked signals significantly differ from the meaningful estimated value, and then the data security can be efficiently assured. Fig. 7 compares the trajectories of USV$_1$ under the proposed and ideal scenarios. Despite a minor initial deviation, the gap diminishes over time, validating the effectiveness of the designed estimation and control methods.

Fig. 8 shows the kinematic and kinetic errors of USV$_1$, i.e., $e_{1,1}$ and $\hat{e}_{1,2}$, and it can be seen that the errors gradually approach 0, which verifies the stability of the error system depicted by

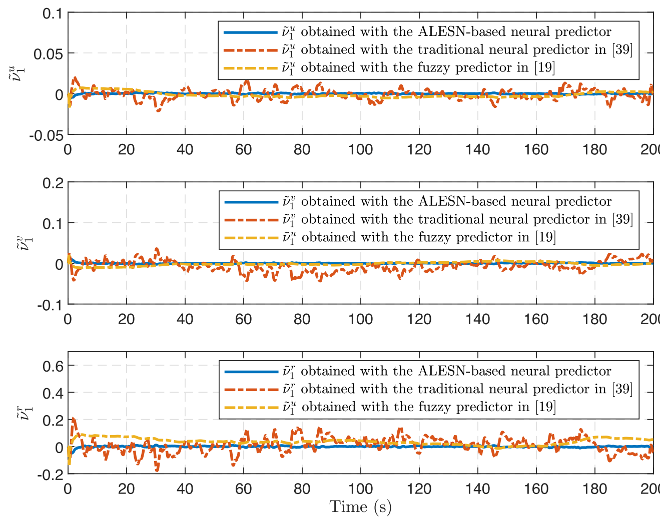


Fig. 12. The prediction errors of $USV_1$ obtained with the three predictors.

(18). Fig. 9 presents that the actual velocity $\nu_1$ closely follows the commanded velocity $\alpha_1$, and thus the effectiveness of the devised control method is further validated. Fig. 10 compares the output of the ALESN, i.e., $F_1(\cdot)$ defined in (9), with $F_1(\nu_1)$. It shows that $F_1(\nu_1)$, which consists of the unknown nonlinear term and positional disturbance, can be well approximated by the ALESN. Furthermore, to assess the effectiveness of the proposed ALESN-based neural predictor, a comparative analysis is conducted against the traditional neural predictor reported in [39], and the fuzzy predictor given in [19], by using the same adaptation gain. As shown in Figs. 11 and 12, it can be observed that the proposed ALESN-based neural predictor outperforms both the traditional neural predictor and the fuzzy predictor in terms of convergence speed and prediction accuracy. Additionally, compared with the traditional ESN predictor, the ALESN-based predictor introduces only a minor increase in computational overhead for weight updates; in contrast to the fuzzy predictor, the ALESN-based predictor leverages a fixed reservoir and a concise update law, ensuring lower overall computational cost. Overall, the ALESN-based neural predictor offers a more efficient and scalable solution compared to both the traditional ESN neural predictor and the fuzzy predictor.

## VI. Conclusion

In this paper, a noncooperative game-based formation control approach for USVs is proposed by taking eavesdropping attacks into account. Specifically, based on a twin-network structure, a privacy-protected estimation method is designed for each USV via utilizing the information received from its neighbors. In the method, given that the masked information is transmitted over the communication network to support action estimation, the data leakage to both eavesdroppers and malicious neighboring USVs is effectively mitigated. Moreover, ALESN-based neural predictors are developed to predict the kinetics of USVs with unknown system parameters. By incorporating ESN with accelerated learning technique, the performance of the predictors can be significantly consolidated. Then, a formation control strategy is devised based on seeking the Nash equilibrium of the constructed noncooperative game, with the aim of minimizing the combined formation and tracking errors. Finally, simulation results demonstrate the feasibility, flexibility and practicability of the proposed USV formation control approach. Future research will aim to develop resilient cooperative control strategies for USV formations operating within more complicated network environments, and incorporate diverse adversarial models to evaluate and enhance the robustness of the system.

## References

[1] S. Han, J. Sun, S. Ding, and L. Zhou, "A potential field-based model predictive target following controller for underactuated unmanned surface vehicles," *IEEE Trans. Veh. Technol.*, vol. 73, no. 10, pp. 14510–14524, Oct. 2024.

[2] Z. Peng, J. Wang, D. Wang, and Q.-L. Han, "An overview of recent advances in coordinated control of multiple autonomous surface vehicles," *IEEE Trans. Ind. Informat.*, vol. 17, no. 2, pp. 732–745, Feb. 2021.

[3] Z. Zhang, B. Huang, B. Zhou, and J. Miao, "An anti-congestion interaction mechanism based leaderless formation control for unmanned surface vehicles with communication interruptions," *IEEE Trans. Veh. Technol.*, vol. 73, no. 11, pp. 16964–16976, Nov. 2024.

[4] G. Zhu, C. Wu, Y. Ma, and S. Hu, "Resource-constrained adaptive neural output feedback security control for networked USVs under dual-channel malicious attacks," *IEEE Trans. Veh. Technol.*, vol. 74, no. 7, pp. 10109–10121, Jul. 2025.

[5] N. Gu, D. Wang, Z. Peng, J. Wang, and Q.-L. Han, "Advances in line-of-sight guidance for path following of autonomous marine vehicles: An overview," *IEEE Trans. Syst., Man, Cybern. Syst.*, vol. 53, no. 1, pp. 12–28, Jan. 2023.

[6] H. Shi, S. He, S.-L. Dai, and C. Dong, "Cooperative learning from neural formation control for uncertain marine surface vehicles with input saturation under switching topology," *IEEE Trans. Transport. Electrific.*, vol. 10, no. 4, pp. 7828–7839, Dec. 2024.

[7] X. Wu, G. Zong, H. Wang, B. Niu, and X. Zhao, "Collision-free distributed adaptive resilient formation control for underactuated USVs subject to intermittent actuator faults and denial-of-service attacks," *IEEE Trans. Veh. Technol.*, vol. 74, no. 9, pp. 13606–13617, Sep. 2025.

[8] P. Yao, R. Zhao, and Q. Zhu, "A hierarchical architecture using biased min-consensus for USV path planning," *IEEE Trans. Veh. Technol.*, vol. 69, no. 9, pp. 9518–9527, Sep. 2020.

[9] J. Pan, T. Han, B. Xiao, and H. Yan, "Predefined-time bipartite time-varying formation tracking control of networked autonomous surface vehicles via hierarchical control approach," *IEEE Trans. Veh. Technol.*, vol. 73, no. 7, pp. 9536–9545, Jul. 2024.

[10] J. Liu, N. Zhang, Y. Li, X. Xie, E. Tian, and J. Cao, "Learning-based event-triggered tracking control for nonlinear networked control systems with unmatched disturbance," *IEEE Trans. Syst., Man, Cybern. Syst.*, vol. 53, no. 5, pp. 3230–3240, May 2023.

[11] L. Cao, Y. Qin, Y. Pan, and H. Liang, "Prescribed performance-based optimal formation control for USVs with position constraints and yaw angle time-varying partial constraints," *IEEE Trans. Intell. Transp. Syst.*, vol. 26, no. 3, pp. 4109–4121, Mar. 2025.

[12] X. Song, C. Wu, H.-K. Lam, X. Wang, and S. Song, "Adaptive fuzzy predefined-time cooperative formation control for multiple USVs with universal global performance constraints," *IEEE Trans. Intell. Transp. Syst.*, vol. 26, no. 7, pp. 10725–10735, Jul. 2025.

[13] Y. Wang, X. Liu, Z. Wu, and C. Dang, "Distributed prescribed-time formation control for underactuated surface vehicles with input saturation: Theory and experiment," *IEEE Trans. Intell. Transp. Syst.*, vol. 25, no. 11, pp. 18611–18623, Nov. 2024.

[14] Z. Chen, X. Nian, and Q. Meng, "Noncooperative formation control in the presence of malicious agents: A game-based strategy," *IEEE Trans. Ind. Informat.*, vol. 20, no. 3, pp. 4972–4981, Mar. 2024.

[15] F. Liu, X. Dong, J. Yu, Y. Hua, Q. Li, and Z. Ren, "Distributed nash equilibrium seeking of $n$-coalition noncooperative games with application to UAV swarms," *IEEE Trans. Netw. Sci. Eng.*, vol. 9, no. 4, pp. 2392–2405, Jul. 2022.

[16] M. Ye, Q.-L. Han, L. Ding, and S. Xu, "Distributed nash equilibrium seeking in games with partial decision information: A survey," *Proc. IEEE*, vol. 111, no. 2, pp. 140–157, Feb. 2023.
[17] W. Wu, Y. Zhang, Z. Jia, J.-G. Lu, and W. Zhang, "Adaptive fault-tolerant fuzzy containment control for networked autonomous surface vehicles: A noncooperative game approach," *IEEE Trans. Fuzzy Syst.*, vol. 32, no. 7, pp. 4192–4204, Jul. 2024.
[18] Y. Zhang, W. Wu, and W. Zhang, "Noncooperative game-based cooperative maneuvering of intelligent surface vehicles via accelerated learning-based neural predictors," *IEEE Trans. Intell. Veh.*, vol. 8, no. 3, pp. 2212–2221, Mar. 2023.
[19] Y. Jiang and Z. Li, "Fully distributed target encircling control of autonomous surface vehicles based on noncooperative games," *IEEE Trans. Intell. Veh.*, vol. 9, no. 4, pp. 4769–4779, Apr. 2024.
[20] J. Liu, Y. Dong, L. Zha, X. Xie, and E. Tian, "Reinforcement learning-based tracking control for networked control systems with DoS attacks," *IEEE Trans. Inf. Forensics Secur.*, vol. 19, pp. 4188–4197, Mar. 2024.
[21] L. Zha, J. Miao, J. Liu, E. Tian, and C. Peng, "Privacy-preserving distributed estimation over sensor networks with multistrategy injection attacks: A chaotic encryption scheme," *IEEE Trans. Syst., Man, Cybern. Syst.*, vol. 55, no. 7, pp. 4969–4978, Jul. 2025.
[22] J. Liu, Y. Deng, L. Zha, X. Xie, and E. Tian, "Event-based privacy-preserving security consensus of multi-agent systems with encryption–decryption mechanism," *Int. J. Robust Nonlinear Control*, vol. 34, no. 7, pp. 4787–4801, 2024.
[23] Y. Sun, K. Yu, A. K. Bashir, and X. Liao, "Bl-IEA: A bit-level image encryption algorithm for cognitive services in intelligent transportation systems," *IEEE Trans. Intell. Transp. Syst.*, vol. 24, no. 1, pp. 1062–1074, Jan. 2023.
[24] Y. Feng, F. Wang, F. Duan, Z. Liu, and Z. Chen, "Anonymous privacy-preserving consensus via mixed encryption communication," *IEEE Trans. Circuits Syst. II, Exp. Briefs*, vol. 69, no. 8, pp. 3445–3449, Aug. 2022.
[25] T. Wu, C. Zhao, and Y.-J. A. Zhang, "Privacy-preserving distributed optimal power flow with partially homomorphic encryption," *IEEE Trans. Smart Grid*, vol. 12, no. 5, pp. 4506–4521, Sep. 2021.
[26] S. Dong, K. Liu, M. Liu, G. Chen, and T. Huang, "Adaptive neural network-quantized tracking control of uncertain unmanned surface vehicles with output constraints," *IEEE Trans. Intell. Veh.*, vol. 9, no. 2, pp. 3293–3304, Feb. 2024.
[27] J.-X. Zhang, T. Yang, and T. Chai, "Neural network control of underactuated surface vehicles with prescribed trajectory tracking performance," *IEEE Trans. Neural Netw. Learn. Syst.*, vol. 35, no. 6, pp. 8026–8039, Jun. 2024.
[28] G. Zhu, Y. Ma, Z. Li, R. Malekian, and M. Sotelo, "Adaptive neural output feedback control for MSVs with predefined performance," *IEEE Trans. Veh. Technol.*, vol. 70, no. 4, pp. 2994–3006, Apr. 2021.
[29] H. Duan, Y. Yuan, and Z. Zeng, "Distributed robust learning control for multiple unmanned surface vessels with fixed-time prescribed performance," *IEEE Trans. Syst., Man, Cybern. Syst.*, vol. 54, no. 2, pp. 787–799, Feb. 2024.
[30] Q. Meng, X. Nian, Y. Chen, and F. Niu, "Noncooperative formation tracking of uavs against multiple cyber-threats: A twin-network approach," *IEEE Trans. Ind. Informat.*, vol. 21, no. 3, pp. 2174–2183, Mar. 2025.
[31] H. Jaeger, "The 'echo state' approach to analysing and training recurrent neural networks-with an erratum note," *German Nat. Res. Center Inf. Technol. GMD Techn. Rep.*, Bonn, Germany, vol. 148, no. 34, Jan. 2001, Art. no. 13.
[32] Y. Jiang, Z. Peng, D. Wang, Y. Yin, and Q.-L. Han, "Cooperative target enclosing of ring-networked underactuated autonomous surface vehicles based on data-driven fuzzy predictors and extended state observers," *IEEE Trans. Fuzzy Syst.*, vol. 30, no. 7, pp. 2515–2528, Jul. 2022.
[33] S.-L. Dai, S. He, Y. Ma, and C. Yuan, "Cooperative learning-based formation control of autonomous marine surface vessels with prescribed performance," *IEEE Trans. Syst., Man, Cybern. Syst.*, vol. 52, no. 4, pp. 2565–2577, Apr. 2022.
[34] J. E. Gaudio, A. M. Annaswamy, J. M. Moreu, M. A. Bolender, and T. E. Gibson, "Accelerated learning with robustness to adversarial regressors," in *Proc. Learn. Dyn. Control*. Jun. 2021, pp. 636–650.
[35] L. Zha, J. Miao, J. Liu, E. Tian, and C. Peng, "Neural predictor-based formation control for unmanned surface vehicles under aperiodic dos attacks: A noncooperative game approach," *IEEE Trans. Veh. Technol.*, vol. 74, no. 10, pp. 15013–15025, Oct. 2025.
[36] K. Ma, G. Hu, and C. J. Spanos, "Distributed energy consumption control via real-time pricing feedback in smart grid," *IEEE Trans. Control Syst. Technol.*, vol. 22, no. 5, pp. 1907–1914, Sep. 2014.
[37] Z. Qu, *Cooperative Control of Dynamical Systems: Applications to Autonomous Vehicles*. Berlin, Germany: Springer, 2009.
[38] R. Skjetne, T. I. Fossen, and P. V. Kokotović, "Adaptive maneuvering, with experiments, for a model ship in a marine control laboratory," *Automatica*, vol. 41, no. 2, pp. 289–298, Feb. 2005.
[39] Z. Peng, J. Wang, and D. Wang, "Containment maneuvering of marine surface vehicles with multiple parameterized paths via spatial-temporal decoupling," *IEEE/ASME Trans. Mechatronics*, vol. 22, no. 2, pp. 1026–1036, Apr. 2017.

**Jinliang Liu** (Senior Member, IEEE) received the Ph.D. degree in control theory and control engineering from the School of Information Science and Technology, Donghua University, Shanghai, China, in 2011. He was a Postdoctoral Research Associate with the School of Automation, Southeast University, Nanjing, China, from 2013 to 2016. He was a Visiting Researcher/Scholar with the Department of Mechanical Engineering, University of Hong Kong, Hong Kong, from 2016 to 2017. He was a Visiting Scholar with the Department of Electrical Engineering, Yeungnam University, Gyeongsan, South Korea, from 2017 to 2018. From 2011 to 2023, he was an Associate Professor and then a Professor with the Nanjing University of Finance and Economics, Nanjing, China. In 2023, he joined the Nanjing University of Information Science and Technology, Nanjing, where he is currently a Professor with the School of Computer Science. His research interests include cyber-physical systems, unmanned systems, privacy preservation, and game theory.

**Zihao Liu** received the B.S. degree in computer science and technology from Changzhou University, Changzhou, China, in 2024. He is currently working toward the M.S. degree in computer science and technology with the College of Computer Science, Nanjing University of Information Science and Technology, Nanjing, China. His research interests include formation control, networked control systems, and neural networks.

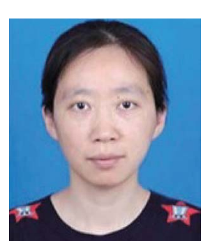

**Yan Li** received the Ph.D. degree in computer science from the University of Science and Technology of China, Hefei, China and City University of Hong Kong, Hong Kong, in 2011. She is currently an Associate Professor with the School of Computer and Artificial Intelligence, Nanjing University of Finance and Economics, Nanjing, China. Her research interests include networked control systems, learning-based algorithms, and software-defined networking.

**Engang Tian** (Senior Member, IEEE) received the B.S. degree in mathematics from Shandong Normal University, Jinan, China, in 2002, the M.Sc. degree in operations research and cybernetics from Nanjing Normal University, Nanjing, China, in 2005, and the Ph.D. degree in control theory and control engineering from Donghua University, Shanghai, China, in 2008. From 2011 to 2012, he was a Postdoctoral Research Fellow with the Hong Kong Polytechnic University, Hong Kong. From 2015 to 2016, he was a Visiting Scholar with the Department of Information Systems and Computing, Brunel University London, U.K. From 2008 to 2018, he was an Associate Professor and then a Professor with the School of Electrical and Automation Engineering, Nanjing Normal University. In 2018, he was appointed as an Eastern Scholar by the Municipal Commission of Education, Shanghai and joined the University of Shanghai for Science and Technology, Shanghai, where he is currently a Professor with the School of Optical-Electrical and Computer Engineering. He has authored or coauthored more than 100 papers in refereed international journals. His research interests include networked control systems, cyber attack, and nonlinear stochastic control and filtering.

**Chen Peng** (Senior Member, IEEE) received the B.S. and M.S. degrees in coal preparation, and the Ph.D. degree in control theory and control engineering from the Chinese University of Mining Technology, Xuzhou, China, in 1996, 1999, and 2002, respectively. From 2002 to 2004, he was a Postdoctoral Research Fellow of applied math with Nanjing Normal University, Nanjing, China. From 2004 to 2005, he was a Research Associate with The University of Hong Kong, Hong Kong. From 2006 to 2007, he was a Visiting Scholar with the Queensland University of Technology, Brisbane, QLD, Australia. From 2010 to 2012, he was a Postdoctoral Research Fellow with Central Queensland University, Rockhampton, QLD, Australia. He is currently a Professor with the School of Mechatronic Engineering and Automation, Shanghai University, Shanghai, China. His research interests include networked control systems, multiagent systems, power systems, and interconnected systems.